

EXPERIMENTAL DETAILS

2.1 BISTATIC SCATTEROMETER MEASUREMENT SYSTEM

An outdoor test bed of an area $10 \times 10 \text{ m}^2$ besides the Department of Physics, IIT (BHU), Varanasi, India was prepared for bistatic scatterometer measurement at different growth stages of rice, wheat, and ladyfinger crop and at different soil moisture content for rough bare soil surface. The location of the study site is described by latitude $25^\circ 13' 52''$ N and longitude $82^\circ 38' 41''$ E. Figure 2.1 shows the bistatic scatterometer system used in our present study. In the bistatic configuration, the transmitter and receiver were placed opposite to each other during the measurement of microwave response of crops/bare soil surface. It has been assembled with PSG high power signal generator (E8257D, 10 MHz to 20 GHz, -20 to 25 dBm), peak and average power sensor (E9327A, 50 MHz to 18 GHz, -60 to 20 dBm), EPM-P series power meter (E4416A, 9 kHz to 110 GHz, -70 to 44 dBm) RF cables (all Agilent Technologies) and microwave power amplifier (83050A, 20 GHz to 50 GHz, gain 20 dBm) (Keysight Technology). The pair of pyramidal horn antennas of X-, C-, and L-bands (Pasternack Technologies) was used for the scatterometer measurements. The bistatic specular scatterometer measurements of the crops/soil were repeated three times for computing average values of the scattering coefficient for each polarization at X-, C-, and L-bands. The specifications of the bistatic scatterometer system are given in Table 2.1. The two pillars of 3 meters each were used to mount a calibrated beam on which the two frames were provided for the antennas, one for the transmitter and other for the receiver, which slide on the calibrated beam. A circular scale for angle measurement from 20° to 60° was provided in the frame for the bistatic scatterometer arrangement.



Figure 2.1 Bistatic scatterometer system

Another plane surface beside the test bed was provided to measure the signal from the aluminium sheet to calibrate the bistatic scatterometer system at every day of measurement. If λ is the wavelength of the transmitted wave, P_t is the transmitted power, G_r and G_t are gain of receiving and the transmitting antennas, R_1 and R_2 are the distance of the transmitting and receiving antenna from the center of the illuminated area, then the power received at the receiver due to the perfectly conducting flat aluminum sheet is given by

$$P_r^{Al} = \frac{P_t G_r G_t \lambda^2}{[(4\pi)^2 (R_1 + R_2)^2]} \quad (2.1)$$

If the reflectivity of a target is $|R_0|^2$ then, the received power can be expressed as

$$P_r = \frac{P_t G_r G_t \lambda^2 |R_0|^2}{[(4\pi)^2 (R_1 + R_2)^2]} \quad (2.2)$$

The reflectivity (r) of the target may be obtained by the equation

$$r = |R_0|^2 = \frac{P_r}{P_r^{At}} \quad (2.3)$$

For the Fraunhofer zone observation, the range ($R = R_1 = R_2$) can be taken large enough so that the R could be considered constant over A_0 (the surface area), the radar equation (Ulaby et al. 1982) reduces to

$$P_r = P_t \lambda^2 \oint_{A_0} \frac{G_r G_t \sigma^0 ds}{[(4\pi)^3 R^4]} \quad (2.4)$$

For the average measurement of the bistatic scattering coefficient of the target such as crop and soil in our case, the bistatic scatterometer system was calibrated with the aluminium sheets.

The power received from a standard target i.e., perfectly flat and smooth aluminium plate is written as

$$P_r^{std} = \frac{P_t G_{tm} G_{rm} \lambda^2}{[(4\pi)^2 (2R)^2]} \quad (2.5)$$

Where G_{tm} and G_{rm} represent the maximum gain of the transmitting and receiving antennas, respectively.

From Equations (2.4) and (2.5), we get

$$\frac{P_r}{P_r^{std}} = \frac{I}{\pi R^2} \quad (2.6)$$

Where $I = \oint_{A_0} \sigma^0 G_{tn} G_{rn} ds$ and $G_{tn} = \frac{G_t}{G_{tm}}$, $G_{rn} = \frac{G_r}{G_{rm}}$

Assuming the bistatic scattering coefficient constant over a 3 dB beamwidth of the antenna beam, we have

$$\sigma^0 = \pi R^2 \frac{P_r}{P_r^{std}} \oint_{A_0} G_{tn} G_{rn} ds \quad (2.7)$$

From Equation (2.6) and (2.7), we have

$$\sigma^0 = \pi R^2 \frac{|R_0|^2}{I_0} \quad (2.8)$$

Where I_0 is the illuminated area of the target. An antenna beam falls on the target surface in the form of an ellipse. Figure 2.2 shows the geometry of the illuminated area on the target by the incidence and reflected beam of microwave. Its minor axis and major axis are given by

$$\text{Minor axis} = 2R \tan\left(\frac{\phi_{az}}{2}\right) \quad (2.9)$$

$$\text{Major axis} = R \sin\left(\frac{\phi_{el}}{2}\right) \left[\sec\left(\theta - \frac{\phi_{el}}{2}\right) + \sec\left(\theta + \frac{\phi_{el}}{2}\right) \right], \quad (2.10)$$

where ϕ_{el} , ϕ_{az} , and θ are elevation, azimuth and look angle of antenna beam, respectively.

Therefore, the illuminated area is given by

$$I_0 = \frac{\pi}{2} R^2 \tan\left(\frac{\phi_{az}}{2}\right) \sin\left(\frac{\phi_{el}}{2}\right) \left[\sec\left(\theta - \frac{\phi_{el}}{2}\right) + \sec\left(\theta + \frac{\phi_{el}}{2}\right) \right] \quad (2.11)$$

Now, substituting the value of I_0 in Equation (2.8), the value of bistatic scattering coefficient is obtained as

$$\sigma^0 = \frac{2|R_0|^2 \cot\left(\frac{\phi_{az}}{2}\right) \operatorname{cosec}\left(\frac{\phi_{el}}{2}\right)}{\sec\left(\theta - \frac{\phi_{el}}{2}\right) + \sec\left(\theta + \frac{\phi_{el}}{2}\right)} \quad (2.12)$$

Therefore, the bistatic scattering coefficient in unit dB can be written as

$$\sigma^0(dB) = 10 \log_{10} \left[\frac{2|R_0|^2 \cot\left(\frac{\phi_{az}}{2}\right) \operatorname{cosec}\left(\frac{\phi_{el}}{2}\right)}{\sec\left(\theta - \frac{\phi_{el}}{2}\right) + \sec\left(\theta + \frac{\phi_{el}}{2}\right)} \right] \quad (2.13)$$

Therefore, knowing the value of the elevation, azimuth, look angle of an antenna, and the reflectivity of the target, we can compute the bistatic scattering coefficient of the target by Equation (2.13).

$$\text{Area of the ellipse} = \frac{\pi}{4} D_1 D_2$$

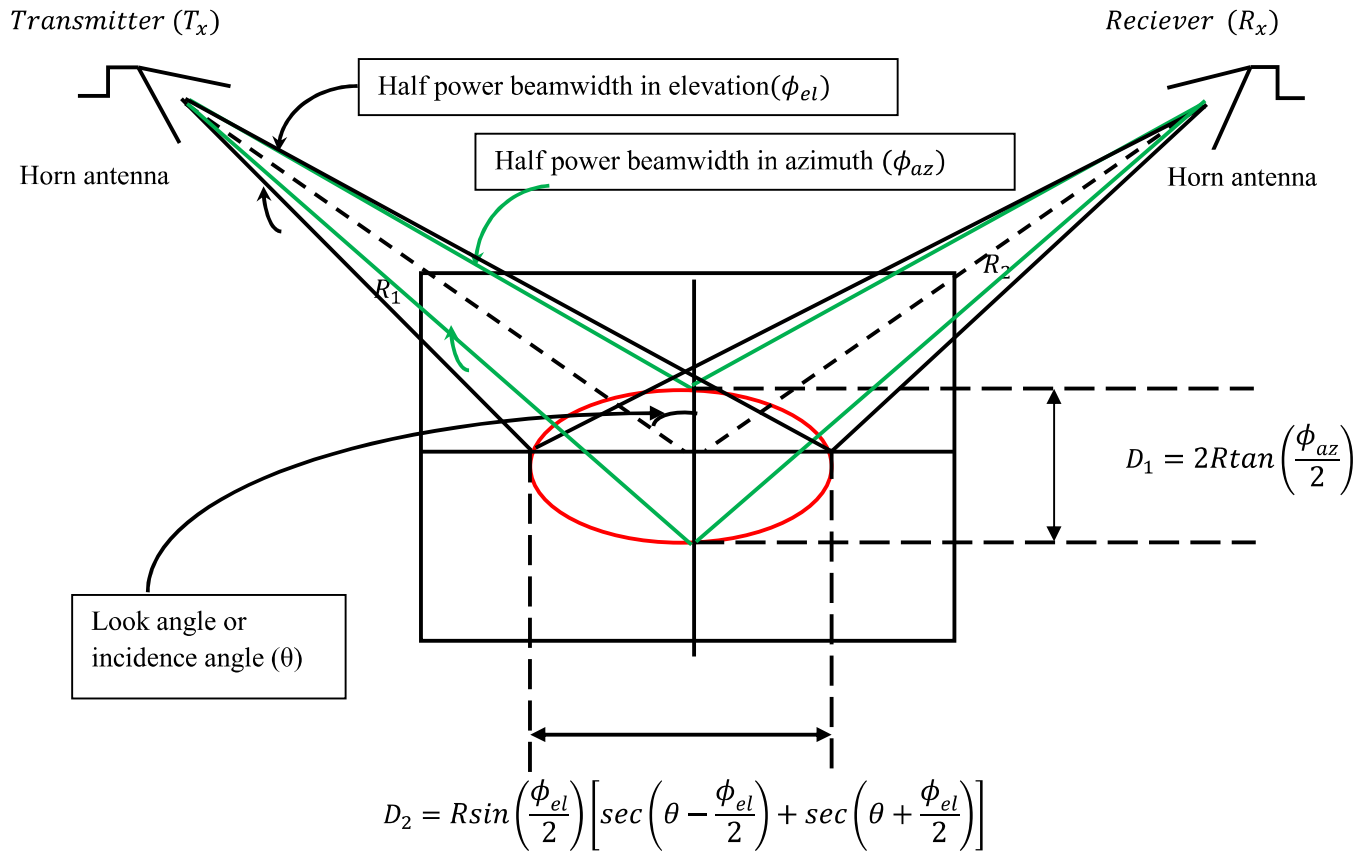


Figure. 2.2 Geometry of the illuminated area by the beam on the target surface

Table 2.1 Specifications of the bistatic scatterometer system

Microwave bands		X- Band	C- Band	L- band
Frequency (GHz)		10	6	2
Beam-width	E-Plane (Degree)	16.5	16.9	45.4
	H-Plane (Degree)	16.1	14.3	64.8
Antenna Type		Dual-Polarised Pyramidal Horn		
Antenna Gain (dB)		20	20	10
Minimum Frequency (GHz)		8.2	4.9	1.7
Maximum Frequency (GHz)		12.4	7.05	2.6
Polarizations		HH, VV, HV		
Incidence angle		10^0 - 60^0 in steps of 10^0		
Platform Height (m)		3.00		
RF generator		E8257D, PSG High Power Signal Generator, 10MHz to 20 GHz (Agilent Technologies)		
Power meter		E4416A, EPM-P Series Power meter, 10MHz to 20 GHz (Agilent Technologies)		
Power sensor		Peak and average power sensor (E9327A, 50 MHz – 18 GHz, -60 to 20 dBm)		
Power amplifier		Microwave system amplifier (83050A, 20 GHz to 50 GHz, gain 20 dBm) (Keysight Technology)		

2.2 CROP GROWTH PARAMETERS MEASUREMENT

2.2.1 Fresh biomass (FBm) and vegetation water content (VWC) measurement

Fresh biomass (FBm) of the crop is defined as the amount of plant weight per meter square of the crop-bed area. The vegetation water content (VWC) is defined as the total water content available in the plant constituents per meter square of the crop-bed area. The crop was grown uniformly in the crop-bed under study. The sampling strategy for the measurement of FBm and VWC depends on the crop type. Two sampling strategies can be adapted to measure the FBm and VWC for a different types of crops.

If the number of plants or bunches/clusters of plants can be determined in 1 m² of the crop-bed like rice and ladyfinger crop, the total number of plants or bunches/clusters was calculated and divided by 100 (10×10 m²) for the determination of the number of plants per m² (plant density). Five different locations in the crop-bed were selected. The total of five plants or bunches/clusters were taken from each different location in the crop-bed for the computation of FBm and VWC. The following equations were used to compute the FBm and VWC (in kg/m²)

$$FBm = (\text{weight of wet plant}) \times \text{plant density} \quad (2.14)$$

$$VWC = (\text{weight of wet plant} - \text{weight of dry palnt}) \times \text{plant density} \quad (2.15)$$

If the number of plants or bunches/clusters of plants can not be determined in 1 m² of the crop-bed like wheat crop, the 10×10 cm² area was selected at five different locations in the crop-bed for sampling. The total plants were pulled out from these five locations in the crop-bed. The small area (10×10 cm²) were selected in the crop-bed because of the limited area available in our crop-bed for observation. The following equations were used to compute the FBm and VWC (in kg/m²)

$$FBm = (\text{weight of wet plant}) \times 100 \quad (2.16)$$

$$VWC = (\text{weight of wet plant} - \text{weight of dry palnt}) \times 100 \quad (2.17)$$

In both cases, a total of five samples was taken for the computation of FBm and VWC from different locations of the crop-bed. The leaves and stalks of plants (five samples) were dried in an oven at 80 °C for 36 hours. These five samples were weighed before and after drying separately. The average of these five samples was taken to compute the overall FBm and VWC.

2.2.2 Leaf area index (LAI) measurement

Leaf area index (LAI) is defined as the ratio of one-sided leaf area to the unit area of the ground surface. In the present thesis, an instrument LAI-2200C Plant Canopy Analyzer (LI-COR, Inc.) was used for the measurement of LAI of the crops. This instrument provides the non-destructive method for the measurement of LAI. It determines LAI by measuring the transmission of radiation through the canopy above and below the canopy (gap fraction method) (Breda 2003). The LAI measurements were taken during sufficient sunlight required for accurate measurement. The LAI measurements were taken at five different locations in all the crop-beds under study. For each location, a single above canopy reading followed by three below-canopies reading was taken for the LAI measurement. The measurements above the canopy serve as a reference. The average of five LAI measurements was taken to compute the average value of the LAI.

2.2.3 Plant height measurement (PH)

A linear wooden scale of 2 m length was used to measure the plant height (PH) in the crop-bed under investigation. The average value of PH was calculated by taking the measurement of plant height at five different locations in the crop-bed.

2.3 SOIL SURFACE PARAMETERS MEASUREMENT

2.3.1 Soil moisture content measurement

The gravimetric moisture content of the soil is defined as the ratio of the weight of water present in the soil to the weight of dry soil. It is expressed as a percentage of soil moisture content. Five random soil samples were collected in aluminum soil containers up to a depth of 15 cm from the soil surface. These soil samples were dried in an oven at 100-110 °C for 24 hours. The soil samples were weighed before and after drying to compute the gravimetric moisture content. The average of gravimetric moisture content of all the five soil samples were taken to calculate the percentage of soil moisture content of the soil surface. The

procedure and requirement to compute the soil moisture content are described as point wise as,

2.3.1.1 Requirements

- i. Oven with 100 -110 °C temperature for drying the soil samples.
- ii. A balance of precision of ± 0.001 g for weighing the soil samples.
- iii. Aluminium soil container and tube Auger for taking soil samples from the ground surface.

2.3.1.2 Procedure to determine the soil moisture content

- i. Taking the soil samples in the soil container from the ground surface up to the depth of 15 cm about a 50 to 200 g. The weight of the wet soil sample was measured.
- ii. The soil sample was placed in the oven at 100 °C for 24 hours or overnight after weighing the wet soil sample.
- iii. After the drying of the soil sample, the weight of the dry soil sample was measured.

2.2.1.3 Soil moisture content computation

The gravimetric soil moisture content (m_g) on a dry weight basis were computed using Equation (2.18) (Singh 2005).

$$m_g = \frac{(\text{weight of wet soil sample}) - (\text{weight of dry soil sample})}{(\text{weight of dry soil sample})} \quad (2.18)$$

2.2.2 Surface roughness measurement

A one-meter long metallic plate painted with the grid of an area of 1 cm² was used for the measurement of soil surface roughness, as shown in Figure 2.3. The metallic plate was pushed into the surface until the grid line reached at the lowest point on the surface. The surface roughness profile was drawn on the metallic plate using an ink marker, as shown in Figure 2.4. The photograph of the surface roughness profile was taken and then later digitized from the photograph. The advantage of this approach is that the equipment is relatively cheap

and easily operated in the field the measurement of soil surface roughness (Oh et al. 1992; Elachi, and Van Zyl 2006).

2.2.2.1 Root mean square (RMS) height (s) measurement

The surface height variation $z(x)$ of a random surface can be considered as the function of horizontal distance (x) across the mean surface. The surface height variations across its horizontal distance can be extracted from the photograph of a rough surface profile. The surface roughness profile is digitized into discrete values $z_i(x_i)$ at an appropriate spacing Δx . This data contains the vertical surface heights (cm) at the horizontal spacing of 1 cm above and below the mean surface height. In the present investigation, 100 data points were acquired from the digitized photograph.

The root mean square height (s) of the discrete one-dimensional surface roughness profile are given as

$$s = \left[\frac{1}{N-1} \left(\sum_1^N z_i^2 - N\bar{z}^2 \right) \right]^{\frac{1}{2}} \quad (2.19)$$

Where N is the number of samples and

$$\bar{z} = \frac{1}{N} \sum_{i=1}^N z_i \quad (2.20)$$

Where \bar{z} is the mean surface of the surface height variation.

2.2.2.2 Auto correlation function and correlation length (l) measurement

The statistical variation of a random surface is characterized by its root mean square height (s) and its autocorrelation function $\rho(\xi)$. The detailed procedure for the measurement of surface height variation $z(x)$ of typical one-dimensional random rough surface profile as a function of horizontal distance (x) is presented in the above subsection.

The surface autocorrelation function is a measure of the degree of correlation between the surface height variation $z(x)$ at a point x on horizontal scale of the surface profile and the surface height variation $z(x + \xi)$ at a point ξ distance from x . The autocorrelation function of the discrete one-dimensional surface can be expressed by Equation (2.21) as

$$\rho(\xi) = \frac{\sum_{i=1}^{N+1-j} z_i z_{j+i-1}}{\sum_{i=1}^N z_i^2} \quad (2.21)$$

Where $\xi = (j - 1) \Delta x$ and j is an integer ≥ 1 .

The correlation length (l) of a rough surface is defined as the displacement ξ for which $\rho(\xi)$ is equal to e^{-1}

$$\rho(l) = e^{-1} \quad (2.22)$$

The value of l is small for a surface with a rapidly varying height profile, whereas for a perfectly smooth surface in which every point is perfectly correlated with every other point, l is infinite. In general, the RMS height (s) is a measure of the vertical roughness of the surface, and correlation length (l) is a measure of the horizontal roughness.

Theoretical surface scattering models have been formulated in terms of the autocorrelation function of the surface $\rho(\xi)$. Several mathematical forms have been used in the literature to describe autocorrelation function $\rho(\xi)$ of the natural surfaces (Oh et al. 1992). For example, these includes

$$\text{Gaussian:} \quad \rho_1(\xi) = \exp\left(-\frac{\xi^2}{l^2}\right) \quad (2.23)$$

$$\text{Exponential:} \quad \rho_2(\xi) = \exp\left(-\sqrt{2}\frac{\xi}{l}\right) \quad (2.24)$$

These theoretical autocorrelation functions do not provide good agreement to measure autocorrelation functions of real surface, particularly for displacements exceeding $\xi = l$. This is the limitation of representing the statistical height variations of real surfaces, which are

responsible for the relatively poor agreement between the theoretically and experimentally observed radar responses to the surface roughness.



Figure 2.3 Metallic plate used for the measurement of soil surface roughness

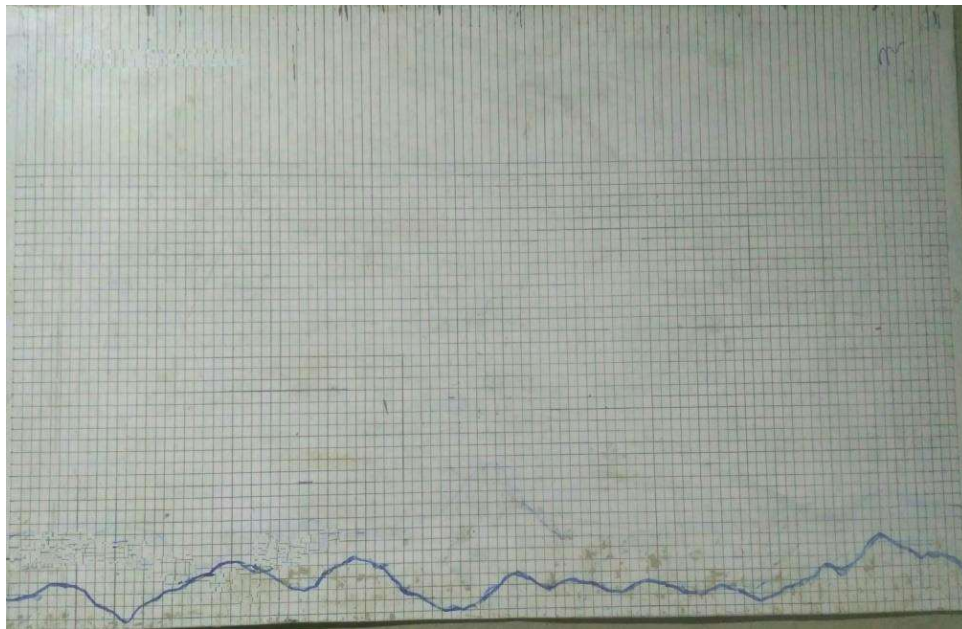


Figure 2.4 The surface roughness profile drawn on the metallic plate using ink marker